AIP | Journal of Applied Physics

Atomic force microscopy-induced electric field in ferroelectric thin films

Biao Wang and C. H. Woo

Citation: J. Appl. Phys. **94**, 4053 (2003); doi: 10.1063/1.1603345
View online: http://dx.doi.org/10.1063/1.1603345
View Table of Contents: http://jap.aip.org/resource/1/JAPIAU/v94/i6
Published by the American Institute of Physics.

Atomic force microscopy-induced electric field in ferroelectric thin films

Biao Wang[a] and C. H. Woo[b]
Department of Mechanical Engineering, The Hong Kong Polytechnic University, Hung Hom, Kowloon, Hong Kong, China

(Received 12 March 2003; accepted 1 July 2003)

The use of atomic force microscopy (AFM) to tailor and image ferroelectric domains in the submicron and nanometer ranges is gaining increasing attention. Many applications have been developed that make use of the superhigh electric field generated by the sharp AFM tip in a local area. In this article, we derive an explicit expression for the AFM-induced electric field in a ferroelectric thin film. Based on a similar approach, we also obtain the depolarization field created by polarization charges using the Green function technique. Based on the expressions derived, the effects of the substrate are discussed. © *2003 American Institute of Physics.*
[DOI: 10.1063/1.1603345]

I. INTRODUCTION

Recent investigations have found that atomic force microscopy (AFM) is useful in tailoring ferroelectric domains in film and bulk ferroelectrics in the submicron and nanometer range. This technique can be used for nanoscopic read/write operations in ferroelectric memory[1,2] and for *in situ* high-resolution ferroelectric domain imaging.[3,4] These applications utilize the superhigh inhomogeneous electric field created by the sharp AFM tip under electric voltage. Despite its obvious appeal, an exact expression for the electric field in the ferroelectric thin films created by the AFM tip and the polarization charges has not been derived.

Hidaka *et al.*[5] proposed an ultrahigh-density memory device based on the AFM domain-imaging technique, and reported that if one manipulates the domain structure by giving direct-current pulses through the nanometer-scale tip, a domain of less than 50 nm in size can form in two opposite directions. Rosenman *et al.*[6] developed a high voltage atomic force microscope that can be used to tailor submicron ferroelectric domains in bulk ferroelectrics, such as $LiNbO_3$, $RbTiPO_4$, and $RbTiOAsO_4$. The expression they used to calculate the electric field created by the AFM tip, however, cannot be applied to thin films, because the effect of the bottom electrode or the substrate is not taken into account. Paruch *et al.*[7] demonstrated that the AFM can be used for precise manipulation of individual ferroelectric domains with size less than 50 nm in ultrahigh density arrays on high-quality $Pb(Zr_{0.2}Ti_{0.8})O_3$ thin films. Control of the domain size was achieved by varying the strength and duration of the voltage pulses used to polarize the materials. Hong *et al.*[8] studied the nucleation and growth of domains during polarization switching in PZT ferroelectric thin film capacitors with Pt top and bottom electrodes by AFM.

The rapid increase in the demand of devices for ultrahigh density information storage, and various domain structures in the submicron and nanometer range, also contribute significant interest to use of the AFM. It is common practice to use the AFM tip as a movable top electrode to create a strongly inhomogeneous electric field in both the plane and thickness directions. To avoid complicated electric field analysis, a slightly modified configuration, namely, an ''AFM tip/top electrode/PZT film/bottom electrode'' was used. To optimize properties for their intended applications, various configurations have been used, including an AFM tip/ferroelectric film/bottom electrode, AFM tip/ferroelectric film/dielectric substrate, and other multilayer structures. It was found that the thickness of the thin film and the dielectric properties of the film and the substrate have very significant effects on the domain switching and retention behavior.

The purpose of this article is to report our analytical solution of the boundary value problem for the electrostatic potential in ferroelectric thin films under action of the AFM tip. Using this solution, the depolarization field and the energy created by the polarization charges for different substrates are then studied.

II. ELECTRIC FIELD NEAR THE AFM TIP

AFMs have been successfully used to imprint stable submicron and nanometer scale ferroelectric domains onto the surface of ferroelectric materials. In ferroelectric domain imaging and tailoring, polarization is produced using the superhigh electric field of the AFM tip, which can be modeled as a single charge Q trapped in a conducting sphere with radius a, corresponding to the tip radius. The electric potential created by the sphere in vacuum is[9]

$$\Phi_0 = \begin{cases} -\dfrac{Q}{4\pi\varepsilon_0 a} & r \leqslant a, \\ -\dfrac{Q}{4\pi\varepsilon_0 r} & r > a, \end{cases} \tag{1}$$

where r is the distance from the charge at the origin to the field point, and ε_0 is the dielectric constant of the vacuum. We consider the AFM tip/ferroelectric thin film/dielectric

[a]On leave from Electro-Optics Technology Center, Harbin Institute of Technology, Harbin, China; electronic mail: wangbiao@hit.edu.cn
[b]Author to whom correspondence should be addressed; electronic mail: chung.woo@polyu.edu.hk

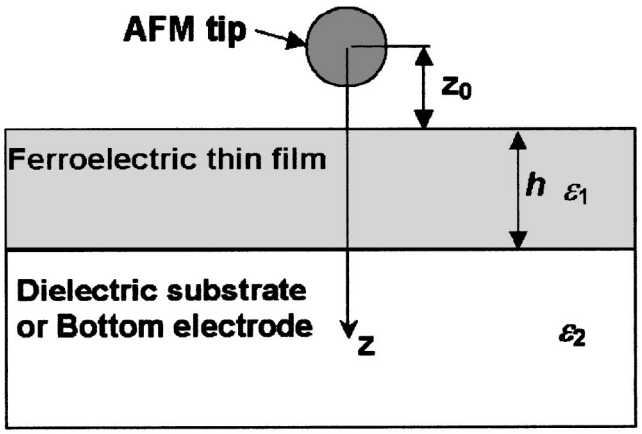

FIG. 1. Schematic of the AFM tip/ferroelectric film/dielectric substrate or/bottom electrode configuration.

substrate configuration in Fig. 1. If the substrate serves as the bottom electrode, one can assume that it has an infinite dielectric constant, i.e., $\varepsilon_2 \to \infty$.

Referring to Fig. 1, we see the electric field is symmetric with respect to the z axis for our problem, and it is convenient to use the cylindrical coordinate system (r,ϕ,z), in which the Laplace equation for the electric potential is

$$\frac{1}{r}\frac{\partial}{\partial r}\left(r\frac{\partial \Phi}{\partial r}\right)+\frac{1}{r^2}\frac{\partial^2 \Phi}{\partial \phi}+\frac{\partial^2 \Phi}{\partial z^2}=0. \tag{2}$$

Separating by means of product functions,

$$\Phi=\Theta(r)\Psi(\phi)\Omega(z), \tag{3}$$

one obtains

$$r\frac{d}{dr}\left(r\frac{d\Theta}{dr}\right)+(k^2r^2-n^2)\Theta=0, \tag{4}$$

$$\frac{d^2\Psi}{d\phi^2}+n^2\Psi=0, \tag{5}$$

$$\frac{d^2\Omega}{dz^2}-k^2\Omega=0, \tag{6}$$

where k and n are the separation parameters. Equation (4) takes the form of the Bessel equation, with the Bessel functions being its solution. For azimuthal symmetry, $n=0$. If the solution extends to infinity radially, so that there are no cylindrical boundaries that might impose restrictions on the radial function $\Theta(r)$, then there are correspondingly no restrictions on k, and the solution can be expressed as an integral over all k:

$$\Theta(r)=\int_0^\infty e^{\pm kz}f(k)J_0(kr)dk, \tag{7}$$

where $J_0(kr)$ is the Bessel function of zeroth order of first kind, and the function $f(k)$ is to be determined by the boundary conditions.

By using the properties of the Bessel functions and the electric potential outside the AFM tip, Eq. (1) can be written as

$$\Phi_0=-\frac{Q}{4\pi\varepsilon_0}\int_0^\infty e^{-k|z|}J_0(kr)dk. \tag{8}$$

The potential of Eq. (8) can be used with the induced potential in Eq. (7) to write the solution for the boundary-value problem. For plane boundaries normal to the z axis (Fig. 1),

$$\Phi_1=-\frac{Q}{4\pi\varepsilon_0}\left[\int_0^\infty e^{-k|z|}J_0(kr)dk+\int_0^\infty A(k)e^{kz}J_0(kr)dk\right],\quad z<z_0, \tag{9}$$

$$\Phi_2=-\frac{Q}{4\pi\varepsilon_0}\left[\int_0^\infty B(k)e^{-kz}J_0(kr)dk+\int_0^\infty C(k)e^{kz}J_0(kr)dk\right],\quad z_0\leqslant z\leqslant z_0+h, \tag{10}$$

$$\Phi_3=-\frac{Q}{4\pi\varepsilon_0}\int_0^\infty D(k)e^{-kz}J_0(kr)dk,\quad z>z_0+h. \tag{11}$$

The undetermined coefficients $A(k)$, $B(k)$, $C(k)$ and $D(k)$ have to be solved to satisfy the boundary conditions for all values of r from 0 to ∞. This requires that the integrands alone satisfy these conditions.[10]

At $z=z_0$, we have $\Phi_1=\Phi_2$, and $\varepsilon_0 d\Phi_1/dz=\varepsilon_1 d\Phi_2/dz$, giving, respectively,

$$e^{-kz_0}+A(k)e^{kz_0}=B(k)e^{-kz_0}+C(k)e^{kz_0} \tag{12}$$

and

$$-\varepsilon_0 e^{-kz_0}+\varepsilon_0 A(k)e^{kz_0}=-\varepsilon_1 B(k)e^{-kz_0}+\varepsilon_1 C(k)e^{kz_0}. \tag{13}$$

At $z=z_0+h$, $\Phi_2=\Phi_3$ and $\varepsilon_1 d\Phi_2/dz=\varepsilon_2 d\Phi_3/dz$, giving, respectively,

$$D(k)e^{-k(z_0+h)}=B(k)e^{-k(z_0+h)}+C(k)e^{k(z_0+h)} \tag{14}$$

and

$$-\varepsilon_2 D(k)e^{-k(z_0+h)}=-\varepsilon_1 B(k)e^{-k(z_0+h)}+\varepsilon_1 C(k)e^{k(z_0+h)}. \tag{15}$$

Solving Eqs. (12)–(15) for $A(k)$, $B(k)$, $C(k)$ and $D(k)$, we have

$$
\begin{aligned}
B(k)&=\frac{2(1+\varepsilon_1/\varepsilon_2)}{(1+\varepsilon_1/\varepsilon_0)(1+\varepsilon_1/\varepsilon_2)-(1-\varepsilon_1/\varepsilon_0)(1-\varepsilon_1/\varepsilon_2)e^{-2kh}},\\
C(k)&=\frac{2(1-\varepsilon_1/\varepsilon_2)e^{-2k(z_0+h)}}{(1-\varepsilon_1/\varepsilon_0)(1-\varepsilon_1/\varepsilon_2)e^{-2kh}-(1+\varepsilon_1/\varepsilon_0)(1+\varepsilon_1/\varepsilon_2)},\\
D(k)&=\frac{4\varepsilon_1/\varepsilon_2}{(1+\varepsilon_1/\varepsilon_0)(1+\varepsilon_1/\varepsilon_2)-(1-\varepsilon_1/\varepsilon_0)(1-\varepsilon_1/\varepsilon_2)e^{-2kh}},\\
A(k)&=[B(k)-1]e^{-2kz_0}+C(k).
\end{aligned}
\tag{16}
$$

Substitution of Eq. (16) into Eqs. (9)–(11) gives the electric potential in the different regions. In the ferroelectric thin film, we have

$$
\begin{aligned}
\Phi_2=&-\frac{2Q}{4\pi\varepsilon_0}\left(\frac{1}{1+\varepsilon_1/\varepsilon_0}\int_0^\infty\frac{J_0(kr)e^{-kz}}{1-\beta e^{-2kh}}dk\right.\\
&-\frac{(1-\varepsilon_1/\varepsilon_2)}{(1+\varepsilon_1/\varepsilon_0)(1+\varepsilon_1/\varepsilon_2)}\\
&\left.\times\int_0^\infty\frac{J_0(kr)e^{k[z-2(z_0+h)]}}{1-\beta e^{-2kh}}dk\right),
\end{aligned}
\tag{17}
$$

where

$$
\beta=\frac{(1-\varepsilon_1/\varepsilon_0)(1-\varepsilon_1/\varepsilon_2)}{(1+\varepsilon_1/\varepsilon_0)(1+\varepsilon_1/\varepsilon_2)}.
$$

Despite the complicated appearance, the integrals in Eq. (17) can be readily evaluated numerically. Noting that $\beta<1$, and expanding the denominator of the integrands with respect to β, we can use the following mathematical identity,

$$
\frac{1}{R}=\frac{1}{\sqrt{z^2+r^2}}=\int_0^\infty e^{-k|z|}J_0(kr)dk,
\tag{18}
$$

to obtain the solution in series form,

$$
\begin{aligned}
\Phi_2=&-\frac{2Q}{4\pi\varepsilon_0}\left[\frac{1}{1+\varepsilon_1/\varepsilon_0}\sum_{n=0}^{\infty}\frac{\beta^n}{[(z+2nh)^2+r^2]^{1/2}}\right.\\
&-\frac{(1-\varepsilon_1/\varepsilon_2)}{(1+\varepsilon_1/\varepsilon_0)(1+\varepsilon_1/\varepsilon_2)}\\
&\left.\times\sum_{n=0}^{\infty}\frac{\beta^n}{[(\hat{z}+2nh)^2+r^2]^{1/2}}\right],
\end{aligned}
\tag{19}
$$

where $\hat{z}=2(z_0+h)-z$.

If the substrate is covered by a bottom electrode and the film is absent, then $\varepsilon_2\to\infty$, $\varepsilon_1=\varepsilon_0$ and Eq. (19) gives

$$
\begin{aligned}
\Phi_2=&-\frac{Q}{4\pi\varepsilon_0}\left(\int_0^\infty J_0(kr)e^{-kz}dk\right.\\
&\left.-\int_0^\infty J_0(kr)e^{k[z-2(z_0+h)]}dk\right)\\
=&-\frac{Q}{4\pi\varepsilon_0}\left(\frac{1}{\sqrt{z^2+r^2}}-\frac{1}{\sqrt{r^2+[z-2(z_0+h)]^2}}\right).
\end{aligned}
\tag{20}
$$

Equation (20) can also be derived via the image method by placing the image charge in the substrate at a specific point (z_0+h) from the substrate surface.

If the thickness of the film approaches infinity, the solution reduces to the semi-infinite dielectric problem, and Eq. (19) gives the same solution as that of Mele.[11]

In the foregoing analysis, the ferroelectric material is treated as an ordinary dielectric without spontaneous polarization. The presence of spontaneous polarization charges in ferroelectric materials induces a depolarization field, which we shall now consider. The substrates of electronic devices may often contain multilayers of different dielectric material. We note that the present method can readily be extended to such cases. By taking the derivative of the electric potential, Eq. (17), with respect to z, the electric field component in the thickness direction is given by

$$
\begin{aligned}
E_z=&-\frac{\partial\Phi_2}{\partial z}\\
=&-\frac{2Q}{4\pi\varepsilon_0}\left(\frac{1}{1+\varepsilon_1/\varepsilon_0}\int_0^\infty\frac{kJ_0(kr)e^{-kz}}{1-\beta e^{-2kh}}dk\right.\\
&+\frac{(1-\varepsilon_1/\varepsilon_2)}{(1+\varepsilon_1/\varepsilon_0)(1+\varepsilon_1/\varepsilon_2)}\\
&\left.\times\int_0^\infty\frac{kJ_0(kr)e^{k[z-2(z_0+h)]}}{1-\beta e^{-2kh}}dk\right).
\end{aligned}
\tag{21}
$$

We consider the electric field in the film for two configurations: (1) the AFM-tip/PZT film/bottom electrode and (2) the AFM-tip/PZT film/MgO substrate. We suppose the dielectric constant of the electrode is infinite, whereas that of the MgO substrate is lower that that of the PZT thin film. Being near the ferroelectric film and the substrate, the electric charge inside the tip depends on the configuration, and can be determined using Eq. (9) by putting Φ_1 equal to the voltage applied at the AFM tip. The material constant is

TABLE I. Numerical parameters.

Dielectric constant of PZT film, ε_1	8.8419×10^{-9} F/m
Dielectric constant of MgO substrate, ε_2	7.1619×10^{-11} F/m
Dielectric constant of vacuum, ε_0	8.8419×10^{-12} F/m
AFM-tip radius, a	20 nm
Thickness of the thin film, h	270 nm
Distance from the center of tip to the surface of the film, z_0	20 nm
Voltage applied to the tip, Φ_1	20 V

shown in Table I, in which the AFM tip is on the thin film. In this case, the charge inside the tip is determined by putting $z=z_0$.

For the two configurations, the electric potentials in the thin film are shown in Fig. 2 as a function of coordinates z and r. The corresponding electric fields are shown in Fig. 3. It is clear that the substrate has a large effect on the electric field distribution in the thin film, which increases for thinner films as shown in Fig. 4.

Ferroelectric domain imaging using contact-mode AFM has recently been proposed as an *in situ* high-resolution probe of the domain structure of ferroelectric materials. Most of these studies were based on the AFM-tip/PZT film/bottom electrode configuration, where a small alternating voltage is applied between the AFM tip and the bottom electrode to induce local piezoelectric movement. The vibration signal of the AFM tip, due to the local piezoelectric activity induced, is collected by a lock-in amplifier. The amplitude of the vibration signal provides information on the magnitude of the piezoelectric coefficient, whereas the phase determines the polarization direction.

Using the piezo-response-imaging technique of AFM, Woo *et al.*[12] measured the bit size versus the voltage applied and pulse width. Despite the large scatter of the data, it is found that the bit size is directly proportional to the pulse voltage. The experimental results are plotted in Fig. 5, together with our theoretical prediction for comparison. It can be seen that the agreement is reasonable at low pulse voltage, within experimental accuracy. However, the calculated value deviates significantly from experimental data at the higher

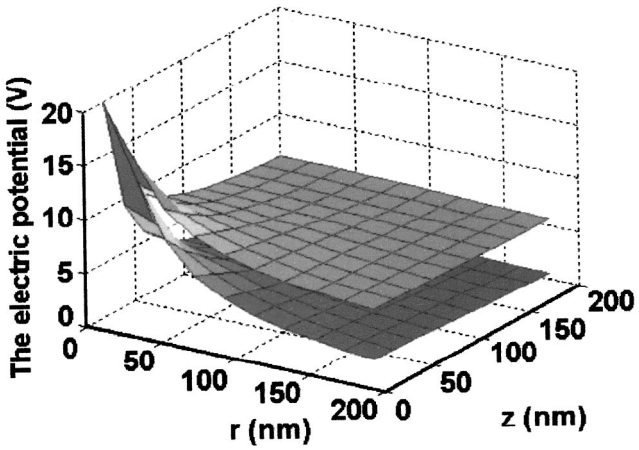

FIG. 2. Electric potential in the thin film as a function of coordinate systems (z, r).

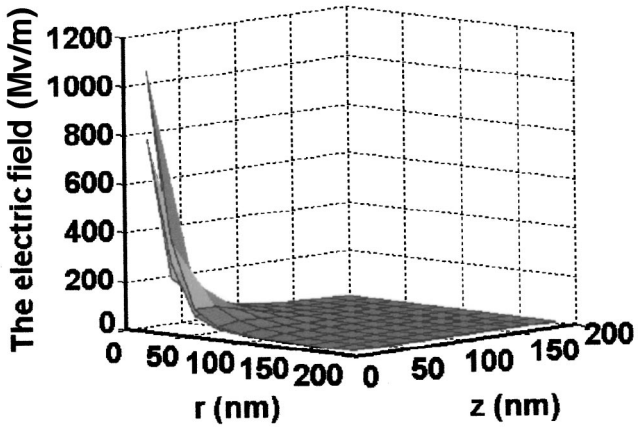

FIG. 3. Electric field in the thin film as a function of coordinate systems (z, r).

pulse voltages. In this calculation, we use 7 MV/m as a universal coercive field for each domain and assume that the field line corresponding to 7 MV/m is the boundary between the dagger type domain developed and the matrix. In this way we can correlate the voltage applied to the tip with the domain size both in the lateral and thickness directions. We note that Woo *et al.*[12] also calculated the bit size versus the voltage applied using an approximate electric field. However, their calculated and the experimental results do no seem to agree.

Our calculation shows that the lateral size of the domain is generally smaller than its depth. For example, when the voltage applied is 16 V, the electric field at the bottom ($z=270$ nm) of the thin film approaches its coercive field, 7 MV/m, whereas in a such case, the lateral size of the surface of the film is about 200 nm.

III. DEPOLARIZATION FIELD OF A FERROELECTRIC DOMAIN IN THIN FILM

The depolarization field in ferroelectric thin films is created by spontaneous polarization charges ρ_P,

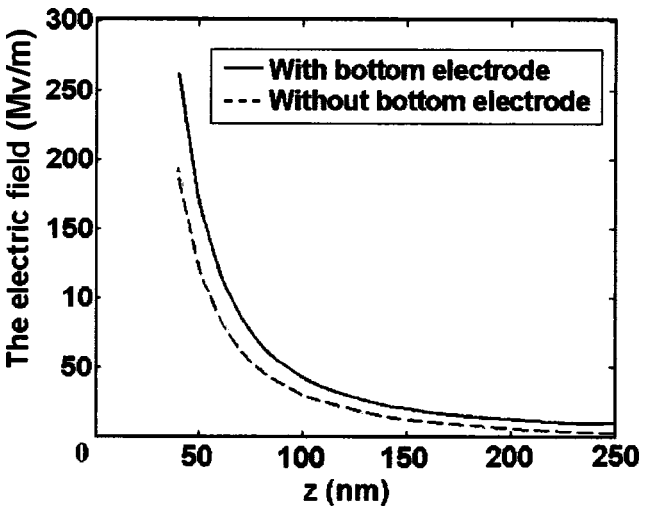

FIG. 4. Electric field in the thin film vs z at $r=0$.

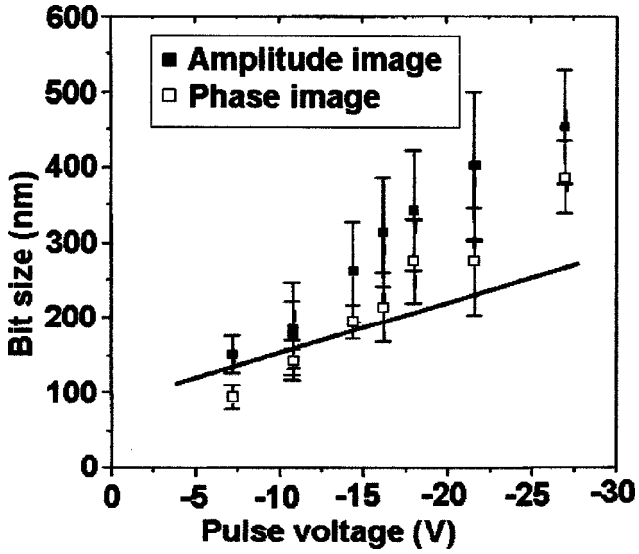

FIG. 5. Experimental data and theoretical prediction of the bit size vs the voltage.

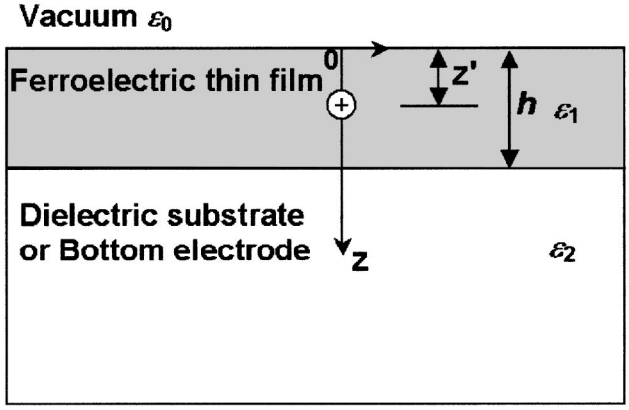

FIG. 6. Schematic of a unit positive charge in the ferroelectric thin film.

$$\rho_P = -\vec{\nabla}\cdot\vec{P} = -P_{i,i}, \tag{22}$$

where P_i is the ith component of spontaneous polarization. The depolarization field induced by the domain can be obtained by integrating, on the boundary of the domain, the Green's function in the thin film for the vacuum/thin film/substrate configuration, which we will derive in the following:

A. Green's function of the vacuum/film/substrate configuration

The solution follows a procedure similar to that in Sec. II, except that a unit positive point charge is in the ferroelectric thin film (Fig. 6) in this case. Using the cylindrical functions to reflect the azimuthal symmetry, for a positive charge at $z=z'$, $r=0$, the electric potentials in the vacuum, the thin film, and dielectric substrate can be expressed, respectively, as

$$G_1 = \frac{1}{4\pi\varepsilon_0}\int_0^\infty M(k)e^{k(Z-z')}J_0(kr)dk, \quad Z<0, \tag{23}$$

$$G_2 = \frac{1}{4\pi\varepsilon_0}\left(\frac{\varepsilon_0}{\varepsilon_1}\int_0^\infty e^{-k|Z-z'|}J_0(kr)dk + \int_0^\infty F(k)e^{k(Z-z')}J_0(kr)dk + \int_0^\infty N(k)e^{-k(Z-z')}J_0(kr)dk\right) \quad 0\leqslant Z\leqslant h \tag{24}$$

$$G_3 = \frac{1}{4\pi\varepsilon_0}\int_0^\infty L(k)e^{-k(Z-z')}J_0(kr)dk, \quad Z>h, \tag{25}$$

where $z'\geqslant 0$. $M(k)$, $N(k)$, $F(k)$ and $L(k)$ are coefficients to be determined by the boundary conditions for all values of r from 0 to ∞. This requires that the integrands alone to satisfy these conditions.[9]

At $Z=0$, $G_1=G_2$ and $\varepsilon_0 dG_1/dz=\varepsilon_1 dG_2/dz$, leading, respectively, to

$$M(k)e^{-kz'} = \frac{\varepsilon_0}{\varepsilon_1}e^{-kz'} + N(k)e^{kz'} + F(k)e^{-kz'}, \tag{26}$$

$$\varepsilon_0 M(k)e^{-kz'} = \varepsilon_0 e^{-kz'} - \varepsilon_1 N(k)e^{kz'} + \varepsilon_1 F(k)e^{-kz'}. \tag{27}$$

At $Z=h$, $G_2=G_3$ and $\varepsilon_1 dG_2/dz=\varepsilon_2 dG_3/dz$, leading, respectively, to

$$L(k)e^{-k(h-z')} = \frac{\varepsilon_0}{\varepsilon_1}e^{-k(h-z')} + N(k)e^{-k(h-z')} + F(k)e^{k(h-z')}, \tag{28}$$

$$-\varepsilon_2 L(k)e^{-k(h-z')} = -\varepsilon_0 e^{-k(h-z')} - \varepsilon_1 N(k)e^{-k(h-z')} + \varepsilon_1 F(k)e^{k(h-z')}. \tag{29}$$

Solving Eqs. (26)–(29) for $M(k)$, $N(k)$, $F(k)$ and $L(k)$ we have

$$N(k) = \frac{(1-\varepsilon_1/\varepsilon_0)(\varepsilon_0/\varepsilon_1-\varepsilon_0/\varepsilon_2)e^{-kh} + (1-\varepsilon_0/\varepsilon_1)(1+\varepsilon_1/\varepsilon_2)e^{k(h-2z')}}{(1+\varepsilon_1/\varepsilon_0)(1+\varepsilon_1/\varepsilon_2)e^{kh} - (1-\varepsilon_1/\varepsilon_0)(1-\varepsilon_1/\varepsilon_2)e^{-kh}},$$

$$F(k) = -\frac{(1+\varepsilon_1/\varepsilon_0)(\varepsilon_0/\varepsilon_1-\varepsilon_0/\varepsilon_2)e^{-k(h-2z')} + (1-\varepsilon_1/\varepsilon_2)(1-\varepsilon_0/\varepsilon_1)e^{-kh}}{(1+\varepsilon_1/\varepsilon_0)(1+\varepsilon_1/\varepsilon_2)e^{kh} - (1-\varepsilon_1/\varepsilon_0)(1-\varepsilon_1/\varepsilon_2)e^{-kh}}. \tag{30}$$

$M(k)$ and $L(k)$ are then obtained by substituting Eqs. (30) into Eqs. (26) and (28). By substituting Eqs. (30) into Eq. (24) one obtains the Green's function in the thin film.

$$\begin{aligned} G_2 &= \frac{1}{4\pi\varepsilon_0}\left(\frac{\varepsilon_0}{\varepsilon_1}\int_0^\infty e^{-k|Z-z'|}J_0(kr)dk \right. \\ &\quad + \int_0^\infty F(k)e^{k(Z-z')}J_0(kr)dk \\ &\quad \left. + \int_0^\infty N(k)e^{-k(Z-z')}J_0(kr)dk\right) \\ &= \frac{1}{4\pi\varepsilon_1}\frac{1}{[(Z-z')^2+r^2]^{1/2}} \\ &\quad + \frac{1}{4\pi\varepsilon_0}\sum_{n=0}^{\infty}\left(\frac{\alpha_1}{[(z_1+2nh)^2+r^2]^{1/2}}\right. \\ &\quad + \frac{\alpha_2}{[(z_2+2nh)^2+r^2]^{1/2}} + \frac{\alpha_3}{[(z_3+2nh)^2+r^2]^{1/2}} \\ &\quad \left. + \frac{\alpha_4}{[(z_4+2nh)^2+r^2]^{1/2}}\right)\beta^n, \end{aligned} \tag{31}$$

where

$$\begin{aligned} \alpha_1 &= \frac{(1-\varepsilon_1/\varepsilon_0)(\varepsilon_0/\varepsilon_1-\varepsilon_0/\varepsilon_2)}{(1+\varepsilon_1/\varepsilon_0)(1+\varepsilon_1/\varepsilon_2)}, \\ \alpha_2 &= \frac{(1-\varepsilon_0/\varepsilon_1)}{(1+\varepsilon_1/\varepsilon_0)}, \\ \alpha_3 &= -\frac{(1-\varepsilon_0/\varepsilon_1)(1-\varepsilon_1/\varepsilon_2)}{(1+\varepsilon_1/\varepsilon_0)(1+\varepsilon_1/\varepsilon_2)} \\ \alpha_4 &= \frac{(\varepsilon_0/\varepsilon_2-\varepsilon_0/\varepsilon_1)}{(1+\varepsilon_1/\varepsilon_2)} \end{aligned} \tag{32}$$

and

$$\begin{aligned} z_1 &= 2h+Z-z', \\ z_2 &= Z+z', \\ z_3 &= 2h-Z+z', \\ z_4 &= 2h-(Z+z'). \end{aligned} \tag{33}$$

Equation (31) gives the electric potential at (Z,r,θ) in the thin film due to a unit positive charge at $Z=z'$, $r=0$. If the unit positive charge is located at (z',r',θ'), the electric potential at (Z,R,θ) is given by Eq. (31) with replacement as follows:

$$r=[R^2+(r')^2-2Rr'\cos(\theta-\theta')]^{1/2}. \tag{34}$$

If the thickness of the film approaches infinity, the problem becomes semi-infinite, and Eq. (31) reduces to the same result as that in Mele's work.[11]

B. Depolarization field of a ferroelectric domain

For a ferroelectric domain with uniform spontaneous polarization, it is clear from Eq. (22) that the charges induced ρ_P are concentrated on the domain boundary. Since the vacuum and substrate are assumed to extend to infinity in our case, one can express, in terms the Green's function, the solution of the electric potential created by ρ_P,

$$\begin{aligned} \Phi(\vec{x}) &= \int\int\int_V G_2(\vec{x},\vec{x}')\rho_P d\nu \\ &= -\int\int\int_V G_2(\vec{x},\vec{x}')P_{i,i'}d\nu \\ &= \int\int\int_V G_{2,i'}(\vec{x},\vec{x}')P_i d\nu \\ &= P_i\int\int_S G_2(\vec{x},\vec{x}')n_i ds, \end{aligned} \tag{35}$$

where S is the surface of the domain, and Eq. (31) gives the Green's function $G_2(\vec{x},\vec{x}')$. In deriving Eq. (35), we have assumed that P_i is restricted in a finite region and the boundary term vanishes. Equation (35) can be used to calculate the depolarization electric potential created by any shape domain by substituting Eq. (31) into it. Under action of the charged AFM tip, we can assume that a cylindrical domain forms normal to the surface from $Z=0$ to a, and that the spontaneous polarization direction is also normal to the surface (z direction). The integration of Eq. (35) reduces to integration on end sections $Z=0$ and a only, except that a delta function multiplied by a constant has to be added to obtain the electric potential inside the upper and lower circular surfaces. It is experimentally found that the surface polarization charges are substantially neutralized due to charge transfer.[13] In such a case, instead of P_i, one has to substitute the remaining charges on the surface for integration on the end section, $z=0$. The depolarization energy of the ferroelectric domain created by the polarization charges is given by

$$U_P = \frac{1}{2}\left[\int\int_{z=0} q_1\Phi(\vec{x})ds + \int\int_{z=a} q_2\Phi(\vec{x})ds\right], \tag{36}$$

where q_1 and q_2 are polarization charges at $z=0$ and a, respectively. If $\vec{P}$ is along the z direction, and the surface polarization charge is not neutralized, one can take $q_1=-P$, $q_2=P$ in Eq. (36), where P is the amplitude of spontaneous polarization, and can be assumed to be $P=30\ \mu\text{C/cm}^2$ for PZT thin films.[13] The materials' constants are shown in Table I. For a cylindrical domain with radius

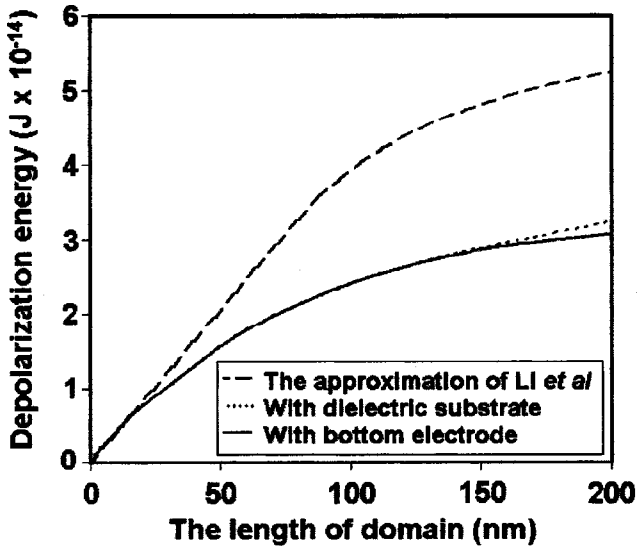

FIG. 7. Depolarization energy vs the length of the cylindrical domain.

$r=80$ nm, the calculated depolarization energy versus length a of the domain is shown in Fig. 7, with a conducting substrate and a dielectric substrate, respectively.

In their domain stability analysis, Li *et al.*[13] obtained an approximate solution for the depolarization energy given by

$$U_{\mathrm{dp}}=f(z/r)\pi r^3\frac{P^2}{2\varepsilon_1},$$

$$f(x)=x \quad \text{for } x<1;$$

$$f(x)=2-x^{-1} \quad \text{for } x>1, \tag{37}$$

which does not reflect the effect of the substrate. The approximation, Eq. (37), is plotted in Fig. 7 for comparison.

IV. CONCLUSIONS

In this article, we have derived explicit expressions for the AFM-generated electric field in ferroelectric thin films. The depolarization field created by the polarization charges in ferroelectrics was also obtained. The effect of the film thickness and of the dielectric properties of the film and the substrate on the switching properties of the near surface domain can be analyzed accordingly.

ACKNOWLEDGMENTS

This project was supported by grants from the Research Grants Council of the Hong Kong Special Administrative Region (PolyU Grant Nos. 5173/01E, 5177/02E, 5309/03E, 5312/03E, and 1/99C), the National Science Foundation of China (Grant Nos. 50232030 and 10172030), and the Natural Science Foundation of Heilongjiang Province.

[1] C. H. Ahn, T. Tybell, J. Antognazza, K. Char, R. H. Hammond, M. R. Beasley, O. Fischer, and J.-M. Triscone, Science **276**, 1100 (1997).
[2] E. B. Cooper, S. R. Manalis, H. Fang, H. Dai, K. Matsumoto, S. C. Minne, T. Hunt, and C. F. Quate, Appl. Phys. Lett. **75**, 3566 (1999).
[3] A. Gruverman, O. Auciello, and H. Tokumoto, Appl. Phys. Lett. **69**, 3191 (1996).
[4] E. L. Colla, S. Hong, D. V. Taylor, A. K. Tagantsev, N. Setter, and K. No, Appl. Phys. Lett. **72**, 2763 (1998).
[5] T. Hidaka *et al.*, Integr. Ferroelectr. **17**, 319 (1997).
[6] G. Rosenman, P. Urenski, A. Agronin, and Y. Rosenwaks, Appl. Phys. Lett. **82**, 103 (2003).
[7] P. Paruch, T. Tybell, and J.-M. Triscone, Appl. Phys. Lett. **79**, 530 (2001).
[8] S. Hong, E. L. Colla, E. Kim, D. V. Taylor, A. K. Tagantsev, P. Muralt, K. No, and N. Setter, J. Appl. Phys. **86**, 607 (1999).
[9] W. K. H. Panofsky and M. Phillips, *Classical Electricity and Magnetism* (Addison–Wesley, Reading, MA, 1962).
[10] W. R. Smythe, *Static and Dynamic Electricity* (McGraw–Hill, New York, 1968).
[11] E. J. Mele, Am. J. Phys. **69**, 557 (2001).
[12] J. Woo, A. Hong, N. Setter, H. Shin, J. Jeon, Y. E. Pak, and K. No, J. Vac. Sci. Technol. B **19**, 818 (2001).
[13] X. Li, A. Mamchik, and I.-W. Chen, Appl. Phys. Lett. **79**, 809 (2001).